# *RXTE* and *BeppoSAX* Observations of MCG −5-23-16: Reflection From Distant Cold Material

B. J. Mattson[1] and K. A. Weaver

*NASA/Goddard Space Flight Center, Laboratory for High Energy Astrophysics, Greenbelt, MD 20771*

## ABSTRACT

We examine the spectral variability of the Seyfert 1.9 galaxy MCG−5-23-16 using *RXTE* and *BeppoSAX* observations spanning 2 years from April 1996 to April 1998. During the first year the X-ray source brightens by a factor of $\sim$ 25% on timescales of days to months. During this time, the reprocessed continuum emission seen with *RXTE* does not respond measurably to the continuum increase. However, by the end of the second year during the *BeppoSAX* epoch the X-ray source has faded again. This time, the reprocessed emission has also faded, indicating that the reprocessed flux has responded to the continuum. If these effects are caused by time delays due to the distance between the X-ray source and the reprocessing region, we derive a light crossing time of between $\sim$ 1 light day and $\sim$ 1.5 light years. This corresponds to a distance of 0.001 pc to 0.55 pc, which implies that the reprocessed emission originates between $3 \times 10^{15}$ cm and $1.6 \times 10^{18}$ cm from the X-ray source. In other words, the reprocessing in MCG−5-23-16 is *not* dominated by the inner regions of a standard accretion disk.

## 1. Introduction

X-ray variability studies can probe the geometry of active galactic nuclei by giving clues about where X-ray reprocessing occurs in relation to the central X-ray source. According to current unified models for Seyfert 1 and Seyfert 2 galaxies (Antonucci 1993), two likely locations for reprocessing are an accretion disk (George & Fabian 1991; Matt, Perola & Piro 1991) and an obscuring molecular torus (Ghisellini, Haardt & Matt 1994; Krolik, Madau & Życki 1994). The X-ray spectral features of reprocessing consist of an Fe K$\alpha$ fluorescence line at $\sim$ 6.4 keV and a "hump" due to Compton reflection, which starts to dominate at $\sim$ 10 keV and is produced by the combined effects of photoelectric absorption and Compton downscattering. If reprocessing occurs in the inner regions of an accretion disk, we expect to see Doppler and relativistically broadened spectral features and small time lags (minutes to hours) between changes in the intrinsic X-ray flux and changes in the iron and reflection components. However, if reprocessing occurs in a larger region such as

[1]Also L-3 Communications Analytics Corporation.

a molecular torus, then the reflected flux is controlled by the time-averaged primary spectrum rather than the instantaneous (observed) one (Malzac and Petrucci 2001), and we might observe a substantial time lag (on the order of years) between changes in the continuum flux and changes in the reflection features.

MCG −5-23-16 (z = 0.008) is an X-ray bright AGN and optically classified as a Seyfert 1.9 galaxy (Véron et al. 1980). The 2 to 10 keV flux varies by at least a factor of 6 between a low state of $\sim 2 \times 10^{-11}$ ergs cm$^{-2}$ s$^{-1}$ and a high state of $\gtrsim 12 \times 10^{-11}$ ergs cm$^{-2}$ s$^{-1}$, as shown in Figure 1. An *ASCA* observation shows a complex, triple-peaked Fe K$\alpha$ line profile (Weaver et al. 1997), which is attributed to a combination of a double-peaked emission line produced in the inner regions of an accretion disk and a narrow emission line from further out in the disk or from elsewhere in the galaxy. The key to the origin of the narrow component is its variability. Based on its line width, we might assume that it originates from a distance that is at least $10^3 R_s$ ($R_s = 2GM/c^2 =$ Schwarzchild radius) from the black hole, which translates into a light crossing time for a $10^8 M_\odot$ black hole of $t \sim 10^5$ s, or a few days.

We present the first broad band spectral variability study of MCG −5-23-16, using data from the *Rossi X-Ray Timing Explorer* (*RXTE*) and *BeppoSAX*. A previous analysis of one of the *RXTE* observations revealed the signature of Compton reflection and confirmed the presence of the broad Fe K line (Weaver, Krolik & Pier 1998). Here we begin with the knowledge that these features exist and we study their variability behavior.

## 2. Data Analysis

### 2.1. *RXTE* Observations

Four observations of MCG −5-23-16 were made by the *RXTE* Proportional Counter Array (PCA): three short 25 ks observations 24 April 1996, 28-29 July 1996 and 10 January 1997, and one long 100 ks observation 27-30 November 1996. The PCA consists of five Proportional Counter Units (PCUs) and is sensitive to energies from 2 to 60 keV. The Standard 2 data for each observation were reduced with the REX (v0.2) script for Ftools (v5.0.1), using the default selection criteria (http://heasarc.gsfc.nasa.gov/docs/xte/recipes/rex.html). Those criteria are: data from layer 1 and from PCUs 0, 1 and 2; times with Earth elevation angle greater than 10°, pointing offset less than 0.02° and electron contamination less than 0.1; and times greater than 30 minutes after the last passage through the South Atlantic Anomaly (SAA). Based on the light curve in Figure 2, the long observation was split into two high states and a low state and spectra of each were extracted separately. This provides six spectra, which we refer to as RX1 (April 1996), RX2 (July 1996), RX3, RX4, and RX5 (November 1996), and RX6 (January 1997). Figure 3 shows the time averaged lightcurve for the six *RXTE* spectra.

The background was estimated using PCABACKEST (v2.1e). We used the L7-240 background

model which incorporates two background components. The "L7" background estimates the internal detector background and is based on housekeeping parameters read directly from the Standard 2 data files. The "240" background models the effects of particles present in the detectors after each SAA passage as a decaying exponential with a half-life of 240 s (http://heasarc.gsfc.nasa.gov/docs/xte/pca_news The response matrix was generated using the Ftool PCARSP (v2.43) with the channel-to-energy matrix from the *RXTE* Guest Observer Facility (GOF) web site (http://heasarc.gsfc.nasa.gov/docs/xte/xte_1st.html). We are confident in the instrument response and background models up to energies of ~25 keV. The background begins to dominate above 25 keV and so we ignore channels with higher energies.

About 11 ks of the 100 ks observation had previously been analyzed by Weaver, Krolik and Pier (1998), who found less Compton reflection in the spectrum of MCG−5-23-16 than our analysis indicates. Since then, the Q6 background models used by Weaver et al. have been retired (http://heasarc.gsfc.nasa.gov/docs/xte/pca_news.html) and the response matrices have changed to reflect the time-dependency of a drift in the detector gain and an increasing xenon fraction in the propane layer of the PCA detectors. In addition, new background models, which refine the L7-240 models, have been made available since our analysis of MCG−5-23-16 was completed. We have examined other data similar to MCG−5-23-16 using both the new and the old L7-240 models and find that the results are consistent. We therefore do not expect the new background models to alter our results. Note however that we do not make specific claims to have reliably measured the absolute amount of reflection in MCG−5-23-16, only changes in the *relative* amount of reflection.

### 2.2. *BeppoSAX* Observation

*BeppoSAX* performed a 100 ks observation of MCG−5-23-16 on 24 April 1998. The Low Energy Concentrator Spectrometer (LECS) and Medium Energy Concentrator Spectrometers (MECS) are imaging telescopes sensitive to 0.1 to 10 keV (LECS) and 1.3 to 10 keV (MECS); whereas, the collimated Phoswich Detector System (PDS) is sensitive to energies from 15 to 300 keV. We only use data from the MECS2 and MECS3, added together. On May 6, 1997 the MECS1 unit developed a fault in its gas cell high voltage supply and has been unavailable since.

We generated images from the LECS and the combined MECS2 and MECS3 data using XSELECT version 2.0 and the event files available through the *BeppoSAX* Science Data Center's web archive (http://www.sdc.asi.it/). The source and background spectra were then extracted based on these images. We obtained a background-subtracted PDS spectra directly from the Data Center's web archive. The source flux remained relatively constant during the *BeppoSAX* observation, so we extract the total spectrum. The response matrices and arf files were obtained from the *BeppoSAX* Guest Observer U.S. Coordination website at GSFC (ftp://heasarc.gsfc.nasa.gov/sax/cal/responses/98_11). We adopt the recommended energy ranges of 0.12 to 4.0 keV for the LECS, 1.65 to 10.5 keV for the MECS, and 15.0 to 220.0 keV for the PDS. We use the full energy band because, although MCG−5-23-16 is heavily absorbed, there are

soft counts in the Rosat band (Mulchaey et al. 1993).

## 3. Results of Spectral Fits

### 3.1. *RXTE* Spectra

The spectrum from each *RXTE* epoch (RX1 to RX6) is fitted from 2.5 to 25 keV with an absorbed Compton reflection model (PEXRAV in XSPEC) plus a Gaussian. PEXRAV simulates the effects of an exponentially cut-off power-law reflected by neutral (except H and He) matter (Magdziarz & Zdziarski 1995). There are seven model parameters, which are the photon index of the intrinsic, underlying power-law ($\Gamma$), the cutoff energy of the power law in keV ($E_c$), the relative amount of reflection ($R$), the redshift ($z$), the abundance of heavy elements in solar units ($Z$), the disk inclination angle ($i$), and the photon flux of the power law at 1 keV in the observer's frame ($A$). The relative amount of reflection is normalized to 1 for the case of an isotropic source above a disk of neutral material ($\Omega = 2\pi$). Adding a Gaussian line (energy in keV, physical width ($\sigma$) in keV and flux in units of photons cm$^{-2}$ s$^{-1}$) and an absorbing column ($N_H$ in units of cm$^{-2}$) yields a total of 12 parameters.

We fix the following values in PEXRAV: $E_c = 100$ keV, $z = 0.008$, $Z = 1.0$ and $\cos i = 0.95$. The cutoff energy is frozen at 100 keV for simplicity since we obtain fairly large errors on this value when fitting the *BeppoSAX* data ($E_c \sim 180 + / - 100$). Perola et al. (2002) find a more conclusive value of $E_c = 147^{+70}_{-40}$. But in any case, fixing the cutoff energy at 147 does not affect our results. The inclination angle of the accretion disk is assumed to be face-on to allow comparison of our results with those of other authors. We also hold the Gaussian width at its best-fitting mean value of $\sigma = 0.24$ keV. This leaves six free parameters: $\Gamma$, $R$, $A$, iron line energy, iron line flux and $N_H$.

The initial spectral results are listed in Table 1. All error bars are 90% confidence for one interesting parameter. Naively fitting the spectra with all parameters free provides the following results: $1.85^{+0.03}_{-0.03}$ (RX2) to $2.00^{+0.02}_{-0.01}$ (RX6), $N_H$ remains approximately constant ($\chi^2/\nu = 0.88/6$ for a constant value) and $R$ changes from $\sim 0.4$ (RX1) to $\sim 0.8$ (RX6). The first five *RXTE* spectra (RX1 through RX5) are similar in shape while RX6 is remarkably softer with a larger apparent amount of reflection and an apparently weaker Fe K line (EW of $\sim 113$ compared to $\sim 125 - 144$). For comparison we show the spectra from the highest and lowest flux states (RX4 and RX6) in Figure 4. The cause of the softening in RX6 is not clear at first glance because there are model degeneracies between $\Gamma$, $N_H$ and $R$ that occur as a result of the way these parameters trade off against each other in the modeling process.

The large modeling degeneracies between the $\Gamma$, $N_H$ and $R$ can lead to false conclusions about spectral variability and so we are challenged to deal with them in a way that allows us to eliminate the degeneracies as much as possble and focus on what we believe is the true variability in the source. But how can we know which parameters represent real changes in the X-ray source and

which are artifacts of the modeling? For example, $R$ has increased substantially in RX6 and this increase is consistent with a systematic error caused by the model degeneracy between $\Gamma$ and $R$. This means that we need to know if there really is a change in $\Gamma$. Unfortunately, when we attempt to measure $\Gamma$ by using only the data between 2.5 and 5.5 keV, to avoid reflection, the errors ($\sim \pm 0.13$) are too large to be useful.

To eliminate systematic errors introduced by the modeling, as well as the instrumental response and background estimations, we calculate the ratio of RX6 to RX4 (Figure 5). The spectral variability is apparent mainly at energies $\lesssim 5.5$ keV. An absorbing column density of $3^{22}$ cm$^{-2}$ begins to cut into the spectrum at just around 5 keV and so this implies that the absorbing column density, rather than $\Gamma$, is what has changed during the high state. Since the energy bandpass of the PCA cuts off at $\sim 3$ keV, the constraints on $N_H$ are actually worse than the statistical errors would indicate and the model compensates for this spectral change by varying (increasing) $\Gamma$ and $R$ to achieve a good statistical fit because of the mathematical degeneracy in the reflection model.[2]

We conclude that a decrease in absorption, rather than a change in the photon index, drives the variability in RX6. We therefore feel confident assuming that $\Gamma$ does not change during the *RXTE* epoch and adopt $\Gamma = 1.88$ (the mean value for RX1 through RX5) for the remaining spectral fits. Table 2 lists the results for the reflection model fixing $\Gamma$ and leaving $N_H$ and $R$ free. The model parameters are plotted in Figure 6. This time the reflection component *decreases* for RX6 ($\chi^2/\nu = 17.42/6$ for R fit to a constant value), which makes more sense compared to the other values and is consistent with a general trend that reflection decreases as the source flux increases (Figure 7). In other words, the reflected flux appears to be lagging behind the changes in the observed continuum.

### 3.2. *BeppoSAX* Results

The *BeppoSAX* data are shown in Figure 8. We use the same model as for *RXTE* except that the Fe K line width is allowed to vary to account for any changes in the line profile. To account for the relative normalization of the instruments, two additional free parameters are added by allowing the MECS and PDS spectra to be offset by a constant from the LECS spectrum. The total number of free parameters is nine: $\Gamma$, $R$, A, iron line energy, iron line width ($\sigma$), iron line flux, $N_H$, the normalization of the MECS relative to LECS ($N_{MECS}$), and the normalization of PDS relative to LECS ($N_{PDS}$).

The two best fits are shown in Table 3, the first with $\Gamma$ free and the second with $\Gamma$ equal to $\Gamma_{(0.12-5.5)}$. The data do not place a good constraint on the reflection fraction (Figure 7), but

[2]This three-way degeneracy is especially a problem for MCG−5-23-16 because it possesses just enough X-ray absorption, a few times $10^{22}$ cm$^{-2}$, to cut the spectrum off near the lower end of the *RXTE* bandpass, which confuses the PCA due to its relatively poor energy resolution. Whether this degeneracy is as severe for other bright Seyfert galaxies has not been tested.

there are notable changes in the spectrum between the *BeppoSAX* and *RXTE* epochs. During the *BeppoSAX* observation, the source has fallen back to its *RXTE* low-flux state, which is close to the historical mean, and $N_H$ has decreased by 40%. At the same time, the Fe K line flux has fallen to almost one-half of its *RXTE* value but the equivalent width is similar to that seen with *RXTE*. This result implies that the features of X-ray reprocessing have tracked the continuum on the longer timescale.

Other authors have commented on the fact that *BeppoSAX* data poorly constrain reflection (Wilkes, et al. 2001; Gliozzi, et al. 2001). Note that Perola et al. (2002) find similar *BeppoSAX* error bars for MCG−5-23-16. We conclude that *RXTE* is more sensitive to reflection than *BeppoSAX*.

## 4. Discussion

Our *RXTE* and *BeppoSAX* observations, combined with data from the literature, show that the X-ray spectrum of MCG−5-23-16 varies on time scales from days to years. The spectral changes are complex and, due to the limited bandpass and resolution of *RXTE*, the derived amounts of absorption and reflection are coupled in a model-dependent fashion via the photon index. From a model-independent comparison of spectra we conclude that a $\sim 20\%$ decrease in X-ray absorption is responsible for a softening of the source in its highest flux state. Changes in absorption on the order of 20% to 80% on timescales of less than 1 year are common in Seyfert 2 galaxies (Risaliti, Elvis & Nicastro 2001). MCG−5-23-16 in particular has shown historical changes in $N_H$ from $\sim 1.5 \times 10^{22}$ $cm^{-2}$ to $\sim 5 \times 10^{22}$ $cm^{-2}$. Taken together, the variability in $N_H$ seen with *RXTE* and *BeppoSAX* spans $1.5 \times 10^{22}$ $cm^{-2}$ to $3 \times 10^{22}$ $cm^{-2}$, which is consistent with its long-term behaviour (Risaliti, Elvis & Nicastro 2001).

We find large degeneracies between the photon index, $N_H$ reflection and Fe K flux that can naively lead to false conclusions about spectral variability. These occur as a result of the way the photon index, nh and reflection trade against each other in the modeling process. We have attempted to deal with them in a way that allows us to eliminate the degeneracies as much as possble and focus on what we believe is the true variability in the source. We believe that our technique has isolated the model-dependent effects and uncovered the true variability.

We find that the relative intensity of the Compton reflected continuum to the directly-viewed continuum decreases as the source brightens on timescales of days to months. To avoid certain degeneracies in the reflection model, we have assumed during the *RXTE* epoch that $\Gamma$ is approximately constant. However, there has been much focus recently on the intrinsic variability of the Seyfert continuum source. In particular, correlated changes between $\Gamma$, $R$ and the 2 to 10 keV flux have been reported for Seyfert galaxies and X-ray binaries (Zdziarski, Lubiński & Smith 1999), in the sense that objects with soft intrinsic spectra show much stronger reflection than do those with hard spectra (although the authors above do not comment whether the flux variability is self-consistent with the location of the proposed reprocessor). In addition, Gilfanov, Churazov &

Revnivtsev (1999) find a strong correlation between $\Gamma$ and R for galactic black hole Cygnus X-1, and Lee et al. (2000) report that the flux and reflection fraction track each other in the Seyfert 1 galaxy MCG −6-30-15. A correlation between $\Gamma$ and $R$ can be explained theoretically by a feedback between the X-ray emitting source and reflecting material. The general idea is that the cold, neutral material (i.e. the reflecting region) emits soft photons which irradiate the X-ray source and serve as seed photons for Compton upscattering.

Because MCG−5-23-16 is fairly heavily absorbed, it is difficult to use the *RXTE* data to search for physical changes in $\Gamma$ and correlations between $\Gamma$ and $R$. On the other hand, it is apparent that $\Gamma$ does decrease between the *RXTE* and *BeppoSAX* epochs 1.5 years apart, which is consistent with the above correlation (since the source flux also decreases between the two epochs). However, during the *RXTE* epoch, any change in $\Gamma$ is *secondary* to the decrease in $N_H$ in terms of producing the observed spectral softening. Indeed, not all studies of Seyfert galaxies show a positive correlation between flux, $\Gamma$ and $R$. Done, Madejski & Życki (2000) find, using *ASCA* and *RXTE* data, that the Seyfert 1 galaxy IC4329a shows a marginal *anti-correlation* between $R$ and source flux. Examining *RXTE* data for Seyfert 2 galaxies, Georgantopoulos and Papadakis (2001) find that although there is a correlation between $\Gamma$ and the $2-10$ keV flux, there is a strong anti-correlation between $R$ and flux. Other work suggests similarly that reflection does not always correlate with flux or photon index. NGC 5548 has shown behavior where $\Gamma$ is correlated with flux but not with $R$ (Chiang et al. 2000), and NGC 5506 shows a tendency for $\Gamma$ to be larger for larger flux states but a weak anticorrelation between flux and $R$ (Lamer, Uttley & McHardy 2000).

Reasons cited above for a lack of the expected correlation between $R$ and flux or $R$ and $\Gamma$ include the possibility that changes in disk inner radial extent and/or ionization structure are small, or that the variability is actually driven by changes in the seed photons that are decoupled from the hard X-ray mechanism. But in most cases the authors assume that there must be an intrinsic correlation between the state of the source (the ionizing spectrum) and the amount of reprocessed emission.

A simple alternative explanation for a relation between the intrinsic flux and $R$ lies in the relative distance between the source and the reprocessor. First of all, if reprocessing occurs in a distant region such as a molecular torus, then the reflected flux is controlled by the time-averaged primary spectrum rather than the observed one (Malzac and Petrucci 2001). Secondly, if there are multiple regions that contribute reflected flux (such as a disk *and* a torus), then the reflected spectrum will comprise a time-average of the portions that vary on short timescales and the portions that vary on long timescales. Depending on which portion dominates, the observed time lag will be weighted toward that emission region. Lamer, Uttley and McHardy (2000) have shown that such a model explains well the lack of a correlation between flux and $R$ in NGC 5506. By examining the relationship of the changes in the spectral features of reprocessing (fluorescence and Compton reflection) to changes in the source flux and continuum variability, it is possible to infer limits on the size(s) of the region(s) that reprocess the X-rays.

There is evidence for complicated X-ray reprocessing in MCG −5-23-16. The ASCA data show an Fe K$\alpha$ line that is triple-peaked with a narrow component and broad, red and blue wings (Weaver et al. 1997). The broad wings are consistent with reprocessing due to an accretion disk near the black hole while the narrow core is consistent with reprocessing in the outer regions of the accretion disk or in the molecular torus. Neither the *RXTE* nor *BeppoSAX* data presented here have the resolution to distinguish these components of the iron line. However, recent *Chandra* observations show that the Fe K line in MCG−5-23-16 has a narrow core with FWHM of <3,000 km s$^{-1}$ (Weaver 2001). The narrow Fe K line suggests a distant reprocessor. There is also evidence for an obscuring torus at other wavelengths. MCG−5-23-16 is heavily reddened in the optical with a weak, broad component to H$\alpha$ (Véron et al. 1980), and there is a broad Pa$\beta$ line in the IR which is clear evidence for a broad line region hidden by dust from our view at optical wavelengths (Goodrich, Veilleux, & Hill 1994). If the narrow line arises in the torus, we expect some of the Compton reflection to arise there as well.

We favor a scenario in which changes in $R$ are due to a time lag following changes in the source flux; although, this picture is somewhat complicated by noticeable changes in the absorbing column. We can place limits on the light-crossing timescale; *RXTE* observations imply a lower limit of $\sim$ 1 light day from the increase in $R$ when the source flux drops to its lowest point between RX3 and RX4, while *BeppoSAX* observations imply an upper limit of $\sim$ 1.5 years from the fact that the Fe K line has tracked the continuum. This places the bulk of the reprocessing between $\sim$ 0.001 pc (or $\sim 150R_S$ for a $10^8 M_\odot$ black hole) and $\sim$ 0.55 pc from the X-ray source.

## 5. Conclusions

We have examined spectral variability in MCG−5-23-16 based on *RXTE* and *BeppoSAX* observations. Based on the time delay between the continuum and reprocessed emission, we derive limits on the response time between changes in the 2 to 10 keV flux and reprocessed emission. The bulk of the reprocessed emission arises from between $\sim$ 1 light day and $\sim$ 1.5 light years, which translates to a region between 0.001 pc ($150R_s$ for a $10^8 M_\odot$ black hole) and 0.55 pc. The bulk of the reprocessed emission must therefore arise in distant cold material, perhaps in the outer regions of an accretion disk.

As part of our analysis, we demonstrate that the choice of photon index may influence the behaviour of the Compton reflection fraction when reflection models are applied without considering the broader complexity of the source, such as the amount of underlying absorption.

We would like to thank Chris Reynolds for helpful discussions and the anonymous referee for providing many useful comments that improved the presentation of this paper. This work was partly supported by NASA grant NAG5-4626.

## REFERENCES

Antonucci, R. 1993, ARA&A, 31, 473

Chiang, J. et al. 2000, ApJ, 528, 292

Done, C., Madejski, G. M., Życki, P. T. 2000, ApJ, 536, 213

George, I. M., and Fabian, A. C. 1991, MNRAS, 249, 352

Georgantopoulos, I. and Papadakis, I. E. 2001, MNRAS, 322, 218

Ghisellini, G., Haardt, F., and Matt, G. 1994, MNRAS, 267, 743

Gilfanov, M., Churazov, E. and Revnivtsev, M. 1999, A&A, 352, 182

Gliozzi, M., Brinkmann, W., Laurent-Muehleisen, S. A., Moran, E. C. and Whalen, J. 2001, AA, 377, 44

Goodrich, R. W., Veilleux, S. and Hill, G. J. 1994, ApJ, 422, 521

Krolik, J. H., Madau, P., and Życki, P. T. 1994 ApJ, 420, L57

Kruper, J. S., Canizares, C. R. and Urry, C. M. 1990, ApJS, 74, 347

Lamer, G., Uttley, P., and McHardy, I. M. 2000, MNRAS, 319, 949

Lee, J. C., Fabian, A. C., Reynolds, C. S., Brandt, W. N. and Iwasawa, K. 2000, MNRAS, 318, 857

Magdziarz, P. and Zdziarski, A. A. 1995, MNRAS, 273, 837

Malzac, J. and Petrucci, P. O. 2001 (astro-ph/0109339)

Markowitz, A., Edelson, R. and Vaughan, S. astro-ph/0308312

Matt, G., Perola, G.C., and Piro, L. 1991, A&A, 247, 25

Mulchaey, J. S., Colbert, E., Wilson, A. S., Mushotzky, R. F. and Weaver, K. A. 1993, ApJ, 414, 144

Mushotzky, R. F. 1982, ApJ, 256, 92

Nandra, K. and Pounds, K. A. 1994, MNRAS, 268, 405

Perola, G. C., Matt, G., Cappi, M., Fiore, F., Guainazzi, M., Maraschi, L., Petrucci, P. O. and Piro, L. 2002, AA, 389, 802

Risaliti, G., Elvis, M., and Nicastro, F. 2001 (astro-ph/0107510)

Singh, K. P., Rao, A. R. and Vahia, M. N. 1992, ApJ, 385, 132

Turner, T. J., Weaver, K. A. Mushotzky, R. F., Holt, S. S. and Madejski, G. M. 1991, ApJ, 381, 85

Véron, P., Lindblad, P. O., Zuiderwijk, E. J., Véron, M. P. and Adam, G. 1980, A&A, 87, 245

Weaver, K. A. 2001, in *The Central Kiloparsec of Starbursts and AGN: The La Palma Connection*, ASP Conf. Proc., Vol. 249. Eds. Knapen, Beckman, Shlosman, and Mahoney (San Francisco: ASP), p. 389.

Weaver, K. A., Krolik, J. H., and Pier, E. A. 1998, ApJ, 498, 213

Weaver, K. A., Yaqoob, T. Mushotzky, R. F., Nousek, J., Hayashi, I. and Koyama, K. 1997, ApJ, 474, 675

Wilkes, B. J., Mathur, S., Fiore, F., Antonelli, A. and Nicastro, F. 2001, ApJ, 549, 248

Zdziarski, A. A., Lubiński, P., Smith, D. A. 1999, MNRAS, 303, L11

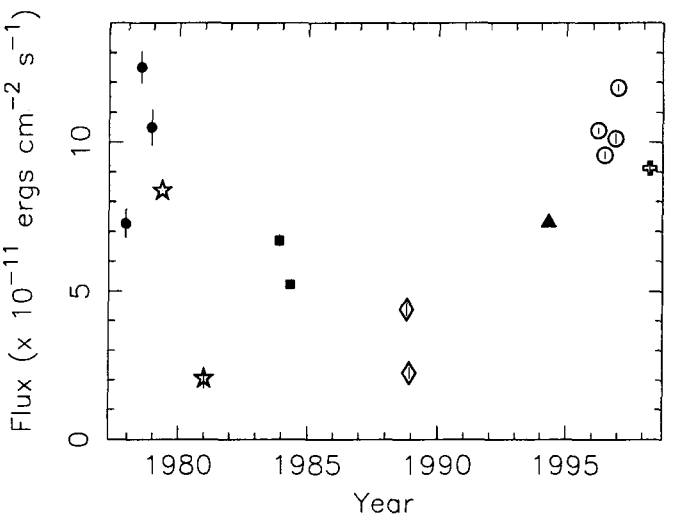


Fig. 1.— The long-term 2-10 keV flux variability of MCG −5-23-16. The symbols represent data from different satellites: filled circles from HEAO1 (Mushotzky 1982), stars from *Einstein* (Turner et al. 1991; Kruper, Canizares & Urry 1990), squares from EXOSAT (Singh, Rao & Vahia 1992), diamonds from *Ginga* (Nandra & Pounds 1994), triangle from *ASCA* (Weaver et al. 1997), open circles from *RXTE* (this paper), and cross from *BeppoSAX* (this paper). A second *ASCA* observation overlaps the third *RXTE* observation.

This preprint was prepared with the AAS LaTeX macros v5.0.

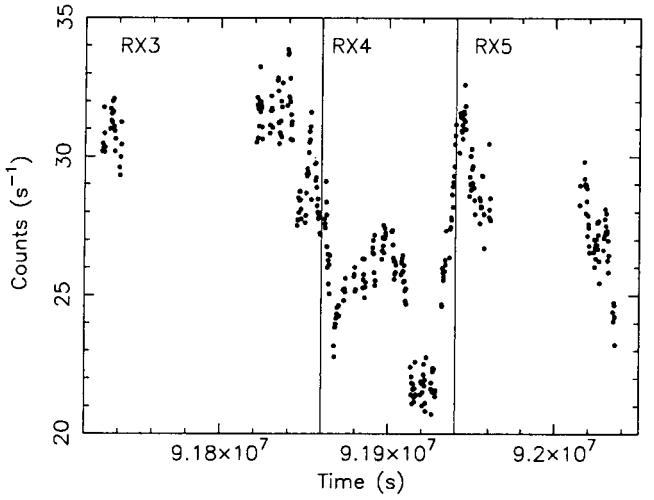


Fig. 2.— *RXTE* PCA lightcurve of the 2 to 10 keV flux for the 100 ks long-look. The vertical lines indicate the temporal divisions that were used for extracting spectra. Mean fluxes for each temporal bin are plotted in Figure 3.

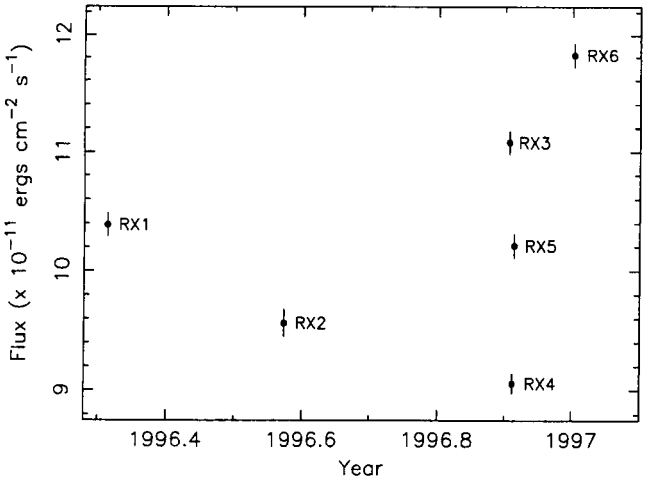


Fig. 3.— Time-averaged lightcurve for the six *RXTE* spectra.

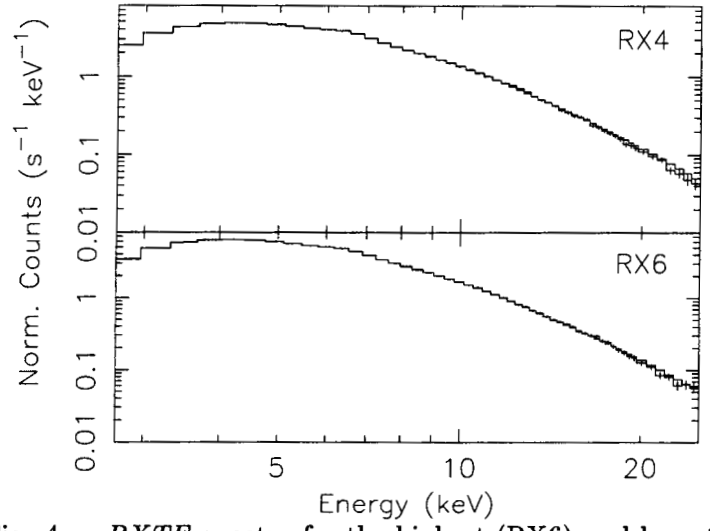


Fig. 4.— *RXTE* spectra for the highest (RX6) and lowest (RX4) flux states.

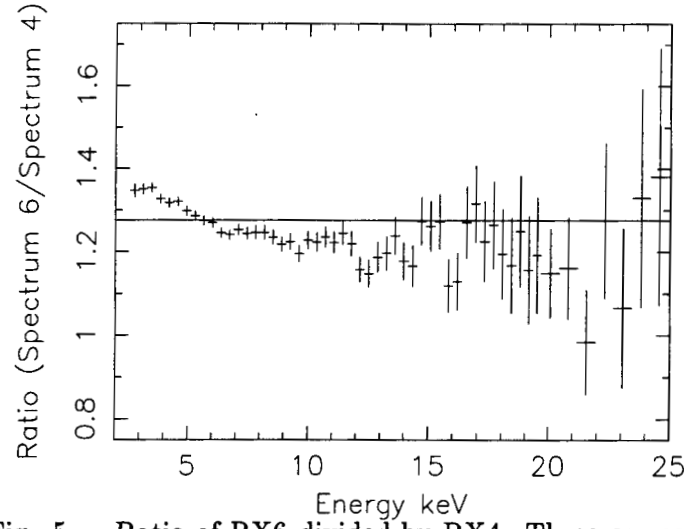


Fig. 5.— Ratio of RX6 divided by RX4. These correspond to the highest and lowest flux states observed with *RXTE*. The straight line represents the best fitting constant to this ratio ($\chi^2/\nu$ = 385.5/65). This plot illustrates the spectral softening below 5 keV caused by a decrease in the absorbing column density between the two observations.

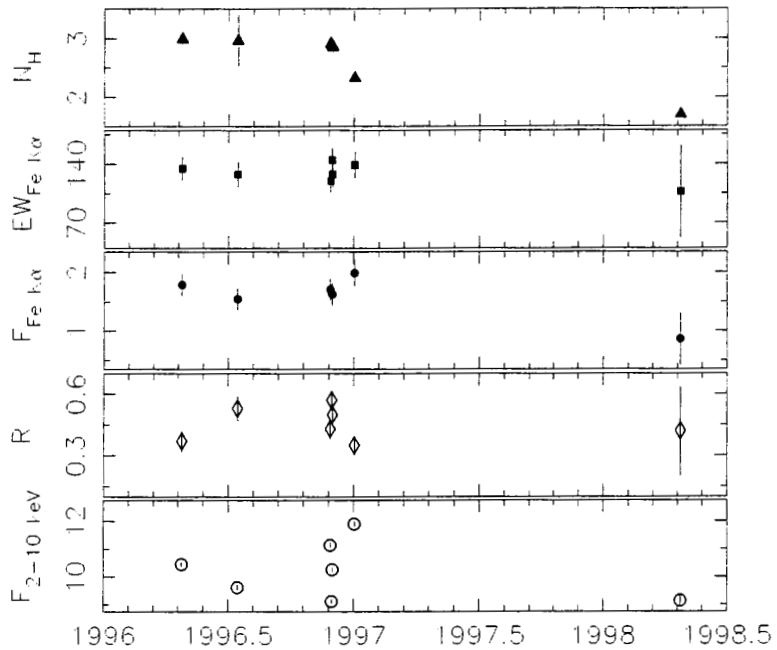


Fig. 6.— Model parameters versus time. From top to bottom are the absorbing column in units of $10^{22}$ cm$^{-2}$, Fe K equivalent width in eV, Fe K line flux in units of $10^{-4}$ photons cm$^{-2}$ s$^{-1}$, reflection fraction ($R$) and $2-10$ keV continuum flux in units of $10^{-11}$ erg cm$^{-2}$ s$^{-1}$, respectively.

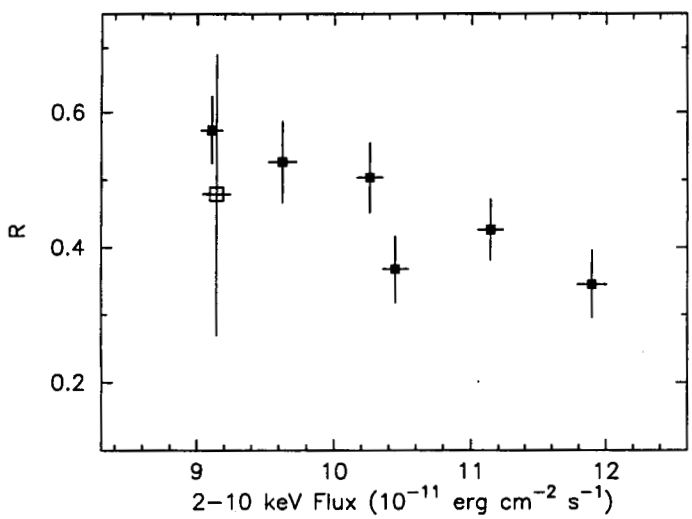


Fig. 7.— The reflection fraction versus 2 to 10 keV continuum flux. The solid squares are the *RXTE* points and the open square is the *BeppoSAX* point.

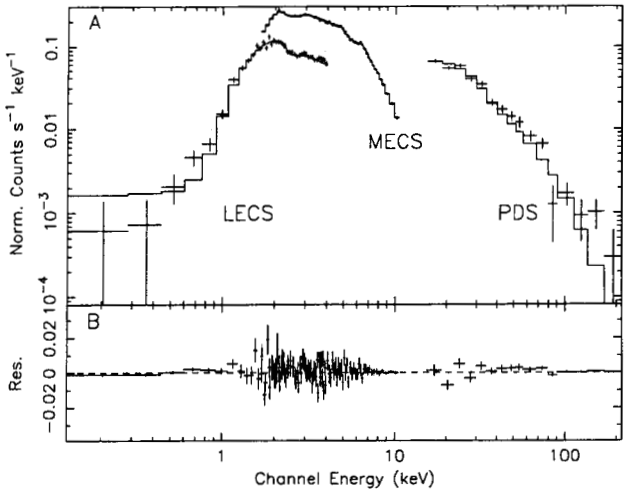


Fig. 8.— *BeppoSAX* data. Panel A shows the data and best-fitting Compton reflection model, plus a Gaussian, folded through the instrumental response. Panel B shows the residuals.

Table 1. RXTE Spectral Fit Results: Fits for the 2 to 25 keV spectra with $\Gamma$ free

| Spectrum[a] | $n_H$[b] | $\Gamma$[c] | R[d] | A[e] | Fe K$\alpha$ Energy[f] | Fe K$\alpha$ Flux[g] | Fe K$\alpha$ $W_{K\alpha}$[h] | $F_{2-10}$[i] | $\chi^2_\nu$[j] |
|---|---|---|---|---|---|---|---|---|---|
| RX1 | $3.04^{+0.17}_{-0.17}$ | $1.89^{+0.03}_{-0.03}$ | $0.40^{+0.11}_{-0.10}$ | $4.35^{+0.22}_{-0.20}$ | $6.33^{+0.05}_{-0.03}$ | $1.71^{+0.19}_{-0.15}$ | $129^{+14}_{-11}$ | $10.44^{+0.51}_{-0.48}$ | 1.32 |
| RX2 | $2.85^{+0.19}_{-0.20}$ | $1.85^{+0.03}_{-0.03}$ | $0.45^{+0.13}_{-0.13}$ | $3.74^{+0.21}_{-0.16}$ | $6.37^{+0.06}_{-0.06}$ | $1.57^{+0.20}_{-0.16}$ | $130^{+17}_{-13}$ | $9.64^{+0.54}_{-0.40}$ | 1.41 |
| RX3 | $2.91^{+0.15}_{-0.16}$ | $1.88^{+0.03}_{-0.03}$ | $0.43^{+0.10}_{-0.09}$ | $4.54^{+0.13}_{-0.20}$ | $6.32^{+0.05}_{-0.05}$ | $1.77^{+0.14}_{-0.20}$ | $125^{+10}_{-14}$ | $11.15^{+0.32}_{-0.48}$ | 1.39 |
| RX4 | $2.84^{+0.15}_{-0.15}$ | $1.87^{+0.03}_{-0.03}$ | $0.55^{+0.11}_{-0.10}$ | $3.60^{+0.16}_{-0.15}$ | $6.39^{+0.04}_{-0.04}$ | $1.63^{+0.13}_{-0.13}$ | $144^{+11}_{-12}$ | $9.11^{+0.40}_{-0.37}$ | 1.11 |
| RX5 | $2.89^{+0.17}_{-0.17}$ | $1.89^{+0.03}_{-0.01}$ | $0.56^{+0.13}_{-0.12}$ | $4.22^{+0.12}_{-0.21}$ | $6.37^{+0.06}_{-0.05}$ | $1.62^{+0.19}_{-0.15}$ | $126^{+15}_{-12}$ | $10.25^{+0.30}_{-0.49}$ | 1.32 |
| RX6 | $2.89^{+0.16}_{-0.16}$ | $2.00^{+0.02}_{-0.01}$ | $0.78^{+0.15}_{-0.13}$ | $5.69^{+0.30}_{-0.10}$ | $6.38^{+0.06}_{-0.06}$ | $1.63^{+0.19}_{-0.18}$ | $113^{+13}_{-13}$ | $11.79^{+0.62}_{-0.21}$ | 0.89 |

[a]The dates for the corresponding sprectra are: RX1, 24 April 1996; RX2, 28-29 July 1996; RX3, RX4, RX5, 27-30 November 1996; RX6, 10 January 1997.

[b]Absorbing column density in units of $10^{22}$ cm$^{-2}$.

[c]Photon index of the intrinsic power-law spectrum. (f) indicates that this parameter was fixed in these fits.

[d]Fraction of reflected flux.

[e]Power-law normalization in units of $10^{-2}$ photons keV$^{-1}$ cm $^{-2}$ s$^{-1}$ at 1 keV.

[f]Energy of the Fe K$\alpha$ line, in units of keV.

[g]Flux of the Fe K$\alpha$ line in units of $10^{-4}$ photons cm$^{-2}$ s$^{-1}$.

[h]Equivalent width of Fe K$\alpha$ line, in units of eV.

[i]2 to 10 keV flux in units of $10^{-11}$ ergs cm$^{-2}$ s$^{-1}$.

[j]Reduced $\chi^2$ for spectral fits, $\nu$ = number of degrees of freedom.

Table 2. RXTE Spectral Fit Results: Fits for the 2 to 25 keV spectra with $\Gamma$ fixed

| Spectrum[a] | $n_H$[b] | $\Gamma$[c] | R[d] | A[e] | Fe K$\alpha$ Energy[f] | Fe K$\alpha$ Flux[g] | Fe K$\alpha$ $W_{K\alpha}$[h] | $F_{2-10}$[i] | $\chi^2_\nu$[j] |
|---|---|---|---|---|---|---|---|---|---|
| RX1 | $2.99^{+0.10}_{-0.10}$ | 1.88 (f) | $0.37^{+0.05}_{-0.05}$ | $4.28^{+0.04}_{-0.04}$ | $6.33^{+0.05}_{-0.05}$ | $1.79^{+0.12}_{-0.19}$ | $135^{+9}_{-14}$ | $10.45^{+0.09}_{-0.09}$ | 1.30 |
| RX2 | $2.96^{+0.11}_{-0.11}$ | 1.88 (f) | $0.53^{+0.06}_{-0.06}$ | $3.89^{+0.04}_{-0.04}$ | $6.38^{+0.06}_{-0.06}$ | $1.55^{+0.15}_{-0.18}$ | $128^{+13}_{-15}$ | $9.62^{+0.10}_{-0.10}$ | 1.40 |
| RX3 | $2.91^{+0.09}_{-0.09}$ | 1.88 (f) | $0.43^{+0.04}_{-0.05}$ | $4.52^{+0.04}_{-0.04}$ | $6.32^{+0.05}_{-0.05}$ | $1.71^{+0.19}_{-0.12}$ | $120^{+14}_{-8}$ | $11.14^{+0.09}_{-0.09}$ | 1.36 |
| RX4 | $2.88^{+0.09}_{-0.09}$ | 1.88 (f) | $0.57^{+0.05}_{-0.05}$ | $3.64^{+0.03}_{-0.03}$ | $6.39^{+0.04}_{-0.04}$ | $1.64^{+0.09}_{-0.16}$ | $145^{+8}_{-14}$ | $9.11^{+0.08}_{-0.08}$ | 1.09 |
| RX5 | $2.82^{+0.10}_{-0.10}$ | 1.88 (f) | $0.50^{+0.05}_{-0.05}$ | $4.11^{+0.04}_{-0.02}$ | $6.36^{+0.05}_{-0.05}$ | $1.63^{+0.19}_{-0.12}$ | $128^{+15}_{-10}$ | $10.26^{+0.09}_{-0.05}$ | 1.31 |
| RX6 | $2.32^{+0.09}_{-0.10}$ | 1.88 (f) | $0.35^{+0.05}_{-0.05}$ | $4.65^{+0.04}_{-0.04}$ | $6.32^{+0.05}_{-0.05}$ | $1.99^{+0.13}_{-0.23}$ | $139^{+9}_{-16}$ | $11.90^{+0.11}_{-0.10}$ | 1.80 |

[a]The dates for the corresponding spectra are: RX1, 24 April 1996; RX2, 28-29 July 1996; RX3, RX4, RX5, 27-30 November 1996; RX6, 10 January 1997.

[b]Absorbing column density in units of $10^{22}$ cm$^{-2}$.

[c]Photon index of the intrinsic power-law spectrum. (f) indicates that this parameter was fixed in these fits.

[d]Fraction of reflected flux.

[e]Power-law normalization in units of $10^{-2}$ photons keV$^{-1}$ cm $^{-2}$ s$^{-1}$ at 1 keV.

[f]Energy of the Fe K$\alpha$ line, in units of keV.

[g]Flux of the Fe K$\alpha$ line in units of $10^{-4}$ photons cm$^{-2}$ s$^{-1}$.

[h]Equivalent width of Fe K$\alpha$ line, in units of eV.

[i]2 to 10 keV flux in units of $10^{-11}$ ergs cm$^{-2}$ s$^{-1}$.

[j]Reduced $\chi^2$ for spectral fits, $\nu$ = number of degrees of freedom.

Table 3. SAX Spectral Fit Results

| Fit | $n_H$[a] | $\Gamma$[b] | R[c] | A[d] | Fe K$\alpha$ Energy[e] | Fe K$\alpha$ $\sigma$[f] | Fe K$\alpha$ Flux[g] | Fe K$\alpha$ $W_{K\alpha}$[h] | $F_{2-10}$[i] | $\chi^2_\nu$[j] |
|---|---|---|---|---|---|---|---|---|---|---|
| 1[k] | $1.66^{+0.06}_{-0.06}$ | $1.73^{+0.02}_{-0.04}$ | $0.22^{+0.37}_{-0.22}$[k] | $2.05^{+0.12}_{-0.10}$ | $6.40^{+0.08}_{-0.08}$ | $0.19^{+0.14}_{-0.19}$[l] | $1.02^{+0.30}_{-0.30}$ | $128^{+38}_{-38}$ | $9.15^{+0.52}_{-0.45}$ | 1.01 |
| 2[m] | $1.70^{+0.04}_{-0.05}$ | 1.77 (f) | $0.48^{+0.22}_{-0.21}$ | $2.12^{+0.04}_{-0.04}$ | $6.40^{+0.08}_{-0.08}$ | $0.18^{+0.15}_{-0.18}$[l] | $0.86^{+0.45}_{-0.22}$ | $107^{+55}_{-28}$ | $9.13^{+0.16}_{-0.18}$ | 1.01 |

[a]Absorbing column density in units of $10^{22}$ cm$^{-2}$.

[b]Photon index of the intrinsic power-law spectrum. (f) indicates that this parameter was fixed in these fits.

[c]Fraction of reflected flux.

[d]Power-law normalization in units of $10^{-2}$ photons keV$^{-1}$ cm $^{-2}$ s$^{-1}$ at 1 keV.

[e]Energy of the Fe K$\alpha$ line, in units of keV.

[f]Physical width of the Fe $K_\alpha$ line, in units of eV.

[g]Flux of the Fe K$\alpha$ line in units of $10^{-4}$ photons cm$^{-2}$ s$^{-1}$.

[h]Equivalent width of Fe K$\alpha$ line, in units of eV.

[i]2 to 10 keV flux from MECS in units of $10^{-11}$ ergs cm$^{-2}$ s$^{-1}$.

[j]Reduced $\chi^2$ for spectral fits, $\nu$ = number of degrees of freedom.

[k]All parameters are free for this fit. The normalization of the MECS spectra relative to the LECS is $N_{MECS} = 1.339^{+0.029}_{-0.028}$, and the normalization of the PDS spectra relative to the LECS is $N_{PDS} = 1.286^{+0.170}_{-0.194}$

[l]A hard limit in the fit parameter was reached before a $\delta\chi^2 = 2.706$.

[m]For this fit, $\Gamma$ is fixed at its 2-5.5 keV value and all other parameters are free. The normalization of the MECS spectra relative to the LECS is $N_{MECS} = 1.338^{+0.031}_{-0.030}$, and the normalization of the PDS spectra relative to the LECS is $N_{PDS} = 1.184^{+0.153}_{-0.129}$